Cite this article
Robinson S, Brown MJ, Matsui H *et al.*
Centrifuge testing to verify scaling of offshore pipeline ploughs.
International Journal of Physical Modelling in Geotechnics,
https://doi.org/10.1680/jphmg.17.00075

Research Article
Paper 1700075
Received 28/11/2017;
Accepted 02/10/2018

Keywords: centrifuge modelling/
offshore engineering/pipes & pipelines

Published with permission by the ICE under the CC-BY 4.0 license.
(http://creativecommons.org/licenses/by/4.0/)

International Journal of Physical Modelling in Geotechnics

ice publishing

Centrifuge testing to verify scaling of offshore pipeline ploughs

Scott Robinson MEng, MIET, FGS, GMICE
Research Associate, School of Science and Engineering, University of Dundee, Fulton Building, Dundee, UK (corresponding author: s.z.robinson@dundee.ac.uk) (Orcid:0000-0001-6949-8239)

Michael John Brown BEng, PhD, GMICE
Reader, School of Science and Engineering, University of Dundee, Fulton Building, Dundee, UK (Orcid:0000-0001-6770-4836)

Hidetake Matsui MEng, MJSCE, MJGS
Research Engineer, Civil Engineering Research Institute, Taisei Corporation, Totsuka, Yokohama, Japan

Andrew Brennan MEng, PhD, GMICE
Senior Lecturer, School of Science and Engineering, University of Dundee, Fulton Building, Dundee, UK (Orcid:0000-0002-8322-0126)

Charles Augarde BSc, MSc, DPhil, CEng, FICE
Professor, Department of Engineering, Durham University, Durham, UK (Orcid:0000-0002-5576-7853)

Will Coombs MEng, PhD
Associate Professor, Department of Engineering, Durham University, Durham, UK (Orcid:0000-0003-2099-1676)

Michael Cortis BEng & Arch (Hons), MSc, PhD
Research Associate, Department of Engineering, Durham University, Durham, UK (Orcid:0000-0003-3190-2130)

Offshore pipeline ploughs have previously been modelled at 1*g* with small 1:50 scale models designed to derive the parameters required for prediction of ploughing in terms of tow force requirements and potential advance rates. This was scaled up to prototype with the validity of the scaling verified through 'modelling of models' and with comparison to typical prototype tow forces but without direct validation. To allow further validation, a long centrifuge box and actuation system was developed for use on a medium-sized beam centrifuge. Previous approaches to 1*g* ploughing were also improved through the use of micro-electro-mechanical systems accelerometers and new low-cost surface scanning techniques. A wide range of ploughing velocities were explored through increasing actuation speeds and the use of pore fluids of different viscosities. The study has shown that although there may be initial concerns over low effective stress scaling issues at 1*g*, in shallow problems with small-scale models, the large deformation nature of the ploughing problem can be replicated with appropriate scaling. This allows the use of 1*g* modelling for more efficient parametric studies for this application and has given further confidence to performance parameters for prototype modelling derived from 1*g* and centrifuge studies.

Notation

A	acceleration change measured from micro-electro-mechanical systems sensor excluding enhanced gravity
C	methylcellulose powder concentration by weight
C_{d}	dynamic or rate effect coefficient
C_{dn}	dimensionless dynamic or rate effect coefficient
C_{s}	dimensionless passive pressure coefficient
C_{w}	plough interface friction ratio
c'	apparent cohesion
c_{v}	coefficient of consolidation
D	plough depth
D_{10}	representative particle size
D_{50}	mean sand particle size
D_{r}	sand relative density
$D_{v=0}$	equivalent plough depth at zero velocity
E'_0	one-dimensional Young's modulus
F	total plough tow force
$F_{v=0}$	plough tow force at the equivalent of zero velocity or determined during dry testing
$F^*_{v=0}$	plough tow force at the equivalent of zero velocity corrected for plough depth changes
F_{w}	interface friction dependent component of tow force
$\boldsymbol{g}$	standard gravitational acceleration
K_{p}	coefficient of passive earth pressure
N	scaling factor
s	dilation potential
V	normalised plough velocity
v	plough velocity
W	plough weight
α	hydroxypropyl methylcellulose (HPMC) viscosity constant
γ	unit weight of the soil
η	methylcellulose dynamic viscosity

1. Introduction

The behaviour of offshore pipeline and cable ploughing lends itself to physical modelling investigation at various scales as existing empirical models to predict plough tow forces and advance rates rely heavily on empirical factors that are normally back figured from small-scale beach tests (Grinsted, 1985; Reece and Grinsted, 1986) or real ploughing campaigns (Cathie and Wintgens, 2001). For instance, interface friction

Downloaded by [UNIVERSITY OF DURHAM] on [15/11/18]. Published with permission by the ICE under the CC-BY license

behaviour for a full-scale plough is often determined by pulling the plough on a beach or in shallow water at low speeds. Even this apparently simple determination is made more difficult as a beach environment may be subject to significant suctions. The plough also typically has a fresh coat of paint that has low interface frictional properties, which is quickly removed on ploughing in granular materials. The plough may also embed and start to generate passive resistance. Therefore, even this simple element (interface friction) of field plough behaviour is not simple to deconvolute from the passive and rate effects that make up the remaining components of plough resistance (Cathie and Wintgens, 2001). This has led to some reluctance to use empirical parameters determined for loose sand that may result in over optimistic predictions of advance rates. The selection of appropriate soil parameters is further complicated where they may only be determined based on site investigation at 1–2 km intervals (OSIG, 2004). One common form of empirical approach used to predict offshore pipeline plough tow forces (F) is that proposed by Cathie and Wintgens (2001)

$$F = C_w W' + C_s \gamma' D^2 + C_d v D^3 \quad (1)$$

where C_w is a dimensionless friction coefficient that may be taken as tan δ, where δ is the soil–steel interface friction angle (Lauder *et al.*, 2013), W' the submerged buoyant plough weight, C_s a dimensionless passive pressure coefficient, γ' the submerged unit weight of the soil, D the depth from the original sand surface to the heel of the plough main share, v the velocity of plough advance and C_d is a dynamic or rate effect coefficient with units of t/(m^3/h).

Due to the potential difficulties in deconvolution and significant costs of full-scale plough deployment, the study of offshore pipeline and cable ploughing (Robinson *et al.*, 2016a) lends itself to scaled physical modelling at 1***g*** where soil beds of known properties can be prepared in a repeatable fashion. Interface behaviour of plough materials can be deconvoluted directly through element testing of steel–sand interfaces in shear and dry sand testing can be used to study the passive resistance behaviour of a plough as ploughing depth increases. Once these elements are understood, the sand can be saturated and tests undertaken at elevated plough rates and various depths in sands of different permeabilities to understand the rate effect component of behaviour (Palmer, 1999). Working at 1***g*** with appropriate sized models has the advantage of simple testing that uses non-specialist equipment that can be undertaken quickly allowing repetition and thus broad parameter consideration.

Limited controlled laboratory testing data for ploughs is available in the literature. Bransby *et al.* (2005) examined the behaviour of pipeline ploughing in layered soils using 1:50 scale model ploughs at 1***g***. Brown *et al.* (2006) proposed that the results of the modelling could be converted to their full-scale equivalent by considering the appropriate scaling laws (Table 1) although this was only verified by calculating scaled-up tow forces that were of similar magnitude to those encountered at full scale. Subsequent to this, 1***g*** model testing facilities were used to study a variety of different ploughing situations and geohazards, for example ploughing in sandwaves (Bransby *et al.*, 2010a, 2010b), across slopes (Bransby *et al.*, 2018), in fibre-reinforced soil (Brown *et al.*, 2015) and varying plough geometry (Lauder *et al.*, 2013) and vibro ploughing (Zefirova *et al.*, 2012) to increase plough efficiency. Further investigation of the scaling effects and proposed scaling for 1***g*** testing (Bransby *et al.*, 2005; Brown *et al.*, 2006) was not undertaken until the research study by Lauder (2011), who used a modelling approach based on tests at 1***g*** with model ploughs at scales of 1:50, 1:25 and 1:10. This previous work was carried out at 1***g*** and at lower stress levels than experienced in the soil surrounding full-size ploughs. To provide support for the output of such 1***g*** testing requires either costly or hard-to-repeat full-size testing, or controlled tests carried out on a geotechnical centrifuge.

The current work has been carried out in order to use centrifuge modelling to verify (or otherwise) plough performance parameters based on 1***g*** testing. It includes a total of 23 centrifuge tests undertaken in loose to very dense sand (Table 2) in both dry and saturated conditions, simulating scaled plough velocities of up to 580 m/h. This paper will describe the development of a large displacement linear actuation system for use in a long centrifuge box mounted on a medium-sized beam centrifuge. This system was developed to undertake both model cable and pipeline ploughing at 50***g***, initially to verify previous scaling assumptions for 1***g*** model testing as part of a wider research study. As well as scaling verification and description of the apparatus, other developments made to

Table 1. Comparison of model scaling factors used for 1***g*** testing and centrifuge modelling

Parameter	Scaling factor for 1*g* testing	Scaling factor for centrifuge testing
Acceleration	1	N
Length	$1/N$	$1/N$
Volume	$1/N^3$	$1/N^3$
Mass	$1/N^3$	$1/N^3$
Stress	$1/N$	1
Force	$1/N^3$	$1/N^2$
Pore fluid viscosity	1	1[a]
Permeability	1	N

[a]Scaling factor is 1 when using water as pore fluid, 100 and 200, respectively, for 100 and 200 cP methylcellulose

Downloaded by [UNIVERSITY OF DURHAM] on [15/11/18]. Published with permission by the ICE under the CC-BY license

Table 2. Model soil properties for the HST95 sand

Property	Value
Permeability[a]: m/s	$1{\cdot}23 \times 10^{-4}$ (17%)
One-dimensional Young's modulus[b]: kN/m^2	647 (53%)
D_{10}: mm	0·10
D_{50}: mm	0·14
Critical state friction angle: degrees	32
Interface friction angle for steel plough: degrees	24
Maximum dry density: kg/m^3	1792
Minimum dry density: kg/m^3	1487

[a]Permeability and E'_0 shown with relative density of sample in parentheses
[b]E'_0 determined at effective stresses relevant to model testing (0·2–0·3 kN/m^2)

assist the study will also be described. This work has been undertaken as part of a joint programme of research, which aims to develop computational techniques to overcome issues with the modelling of large offshore deformation operations such as cable and pipeline ploughing (Cortis *et al.*, 2017).

2. Scaling laws adopted for 1*g* testing

The scaling laws for 1***g*** model plough testing as initially proposed by Bransby *et al.* (2005) and verified as of appropriate magnitude against field experience by Brown *et al.* (2006) are now discussed. The scaling adopted for 1:50 scale is that lengths are reduced by a factor of 50, areas by a factor of 50^2 and volumes by a factor of 50^3. As the model tests are undertaken at 1***g*** the unit weight of the soil is identical to full scale so effective stresses will be reduced by a factor of 50 due to the shallow reduced scale trenching depth, which at field scale may be 1·5–2 m deep typically (for a single pass of the plough). If it is assumed that a Coulomb failure envelope (with $c' = 0$ kPa and zero dilation) describes the soil failure envelope then there will be a 50 times reduction in shear strength in the model compared to the prototype. Additionally, the weight of soil above the plough share in the model will be reduced by a factor of 50^3. As the tow forces measured during a test are either proportional to the projected area of the plough multiplied by a shear stress or due to soil self-weight, in either case, the model forces will need to be multiplied by 50^3 to recreate full-scale behaviour. This is because the area will be reduced by 50^2 and the shear stress by a factor of 50, thus the model tow forces will be $1/50^3$ ($= (1/50^2) \times (1/50)$) times the field tow forces (Brown *et al.*, 2006). The scaling adopted for 1***g*** testing is summarised in column one of Table 1.

These scaling laws were adopted by Lauder *et al.* (2012), who looked at the origins of the empirical correction factors (C_w, C_s and C_d) in Equation 1 in some detail. When investigating the origins of the passive resistance term C_s through dry ploughing in three different sands at various relative densities and plough depths it was discovered that the value of C_s did not vary significantly with relative density (12·2–15·2). This was in contrast to C_s varying from 5 (loose sand) to 20 (very dense sand) as previously back figured from full-scale ploughing (Cathie and Wintgens, 2001). Similarly, the rate effect or dynamic term C_d was found to increase at a reduced rate with permeability than that determined in the field (Lauder *et al.*, 2013). As the 1***g*** testing was undertaken at very low effective stresses relative to the field (typical trench depths of 32 mm compared to 1·6 m prototype) it might be anticipated that dilation would be increased and peak friction angles would be elevated resulting in significant variation of both C_s and C_d over and above that seen in the field. As this was not the case, and no previous consistent verification of scaling had been undertaken, a 'modelling of models' study was undertaken by Lauder (2011), which involved the testing of models ploughs at scales of 1:50, 1:25 and 1:10. Due to the size and difficulties of preparing samples for the 1:10 scale plough along with limited pull distances only dry tests were undertaken at this scale limiting the verification of scaling of the rate effects. Results of this study (in loose and dense sands) are shown in Figure 1 where the plough tow forces scaled up to prototype using the scaling factors in Table 1 are compared with the Cathie and Wintgens (2001) approach using the factors for C_s derived from 1:50 scale 1***g*** model testing. The modelling of models suggests that the values of C_s derived from 1:50 scale tests are appropriate for predicting behaviour at 1:10 scale and potentially at prototype scale. It is also clear that anecdotal concerns over adopting excessively low C_s values in loose sand are justified, as measured data suggests this under predicts tow

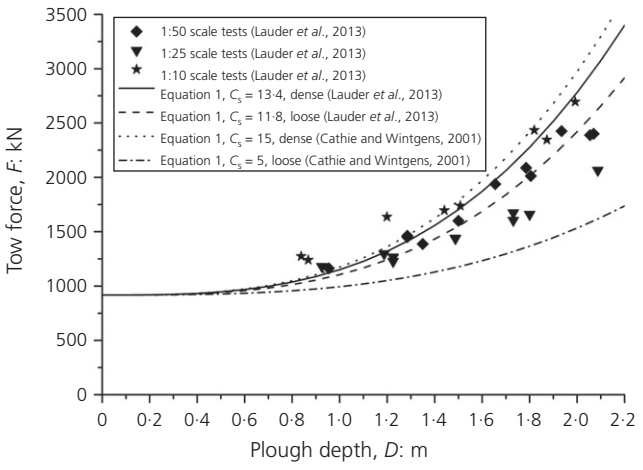

Figure 1. Comparison of the tow force–depth predictions based on modelling of models (Lauder *et al.*, 2013) with those based on parameters determined for field studies (Cathie and Wintgens, 2001). Test shown in loose and dense dry HST95 sand at prototype scale

Downloaded by [UNIVERSITY OF DURHAM] on [15/11/18]. Published with permission by the ICE under the CC-BY license

forces significantly. Further discussion of this difference and the appropriateness of adopting 1***g*** testing for ploughing are given in Lauder *et al.* (2013) and Lauder and Brown (2014) although it is acknowledged that further verification of the scaling and assumptions made is required.

As part of the study by Lauder *et al.* (2013) and with prompting from MF Randolph (2012, personal correspondence) the form of the Cathie and Wintgens (2001) approach was also modified to make the C_d term dimensionless

$$2. \quad F = \left(C_w W' + C_s \gamma' D^3\right)\left(1 + C_{dn}\frac{svD}{c_v}\right)$$

where C_{dn} is a non-dimensional form of rate effect coefficient, s the dilation potential (Palmer, 1999), a method for the determination of which is described in Lauder *et al.* (2012) and c_v the coefficient of consolidation, which was determined at appropriate stress levels for the model testing (Lauder and Brown, 2014). The results in Figure 2 present normalised tow forces ($F/F_{v=0}$, where $F_{v=0}$ is based on the equivalent target depth tow force in dry sand, which has effectively zero rate effect) found during 1:50 scale and 1:25 scale ploughing tests. For the velocities associated with the 1:50 scale tests (0–240 m/h) there is good agreement at both scales but there appears to be some non-linearity in the 1:25 scale tests (>250 m/h), which is also shown by the variation in C_{dn}. Based on these results and the lack of verification at the upper model scale of 1:10 it would appear necessary for further verification of the scaling of rate dependency especially at increased ploughing rates. Further verification of the 1***g*** scaling assumptions for both 'static' and rate effect behaviour is therefore necessary and is addressed in this paper through centrifuge testing.

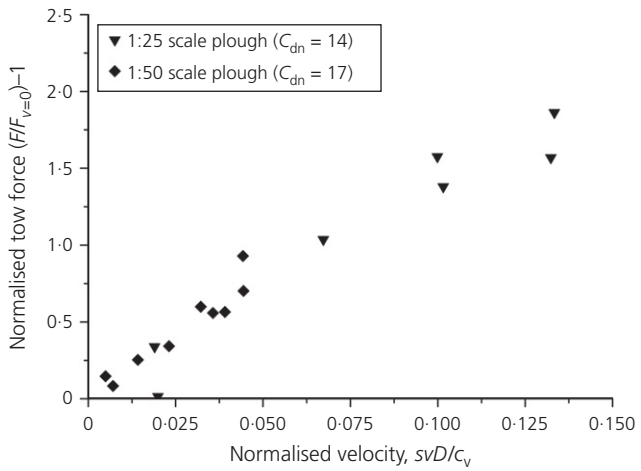

Figure 2. Comparison of rate effects during ploughing tests performed in water saturated sand at 1:50 and 1:20 scale as modified from Lauder *et al.* (2013) (HST95, D_r = 53%)

3. Development of new centrifuge apparatus

3.1 Model box and actuation system

Due to the comparatively large displacements required to reach steady state when testing model ploughs (approximately three ploughs share lengths where the share length at model scale was 110 mm in this study), the existing centrifuge model containers available were unable to accommodate ploughing. To overcome this, a new enlarged 1·6 m long model container was designed and fabricated. The container was fabricated from 50 mm thick steel plate and cast acrylic in order to ensure that it had sufficient rigidity to meet the deflection limits suggested by Garnier *et al.* (2007) to prevent soil disturbance during spin up. The centrifuge container consisted of two end plates of external dimension 650×400 mm machined from 50 mm thick steel. The sides of the container were made from 50 mm thick acrylic sheets 650×1600 mm. These were braced along the top edge by a solid steel beam element 50×50 mm and at mid-length by a vertically orientated solid steel element 50×50 mm to further minimise bending (Figure 3(a)). The edge beams were themselves braced together across the top of the container at least every 500 mm by 50×15 mm aluminium bars, which form part of the actuator for ploughing.

The actuator consists of a moving instrumentation platform mounted on four pairs of two Igus Drylin WJ200QM-01-16 linear bearings (two bearings at each corner of the platform) each with a vertical capacity of 2·1 kN running on Igus WSQ-16 linear rails attached to a rigid frame (Figure 3(c)). These bearings are used due to their low friction coefficient and also due to the fact that their lubricant-free operation prevents performance issues related to the ingress of sand particles. The platform actuation is provided by a belt system using two Brecoflex 25AT10 steel-reinforced polymer belts on either side of the container each with a tensile capacity of 3·5 kN, driven by a Parvalux SD12-LWS high torque 220 V DC motor (capacity of 63 N m at 13 r/min). At each end of the container, the drive belts are connected to 47 mm diameter AT10 pulleys mounted on a 20 mm diameter steel drive shaft attached to rotary bearings on the frame. To make the design as compact as possible, the belts and pulleys are housed within the two structural aluminium channels (100 mm × 50 mm × 6 mm), which make up the frame. At the motor end, a further motor drive belt with a 95 mm diameter pulley on the drive shaft and a 47 mm diameter pulley on the motor provides the actuation. The combination of pulleys used provides an overall gear ratio of 2 in order to reduce the torque on the motor to

Downloaded by [UNIVERSITY OF DURHAM] on [15/11/18]. Published with permission by the ICE under the CC-BY license

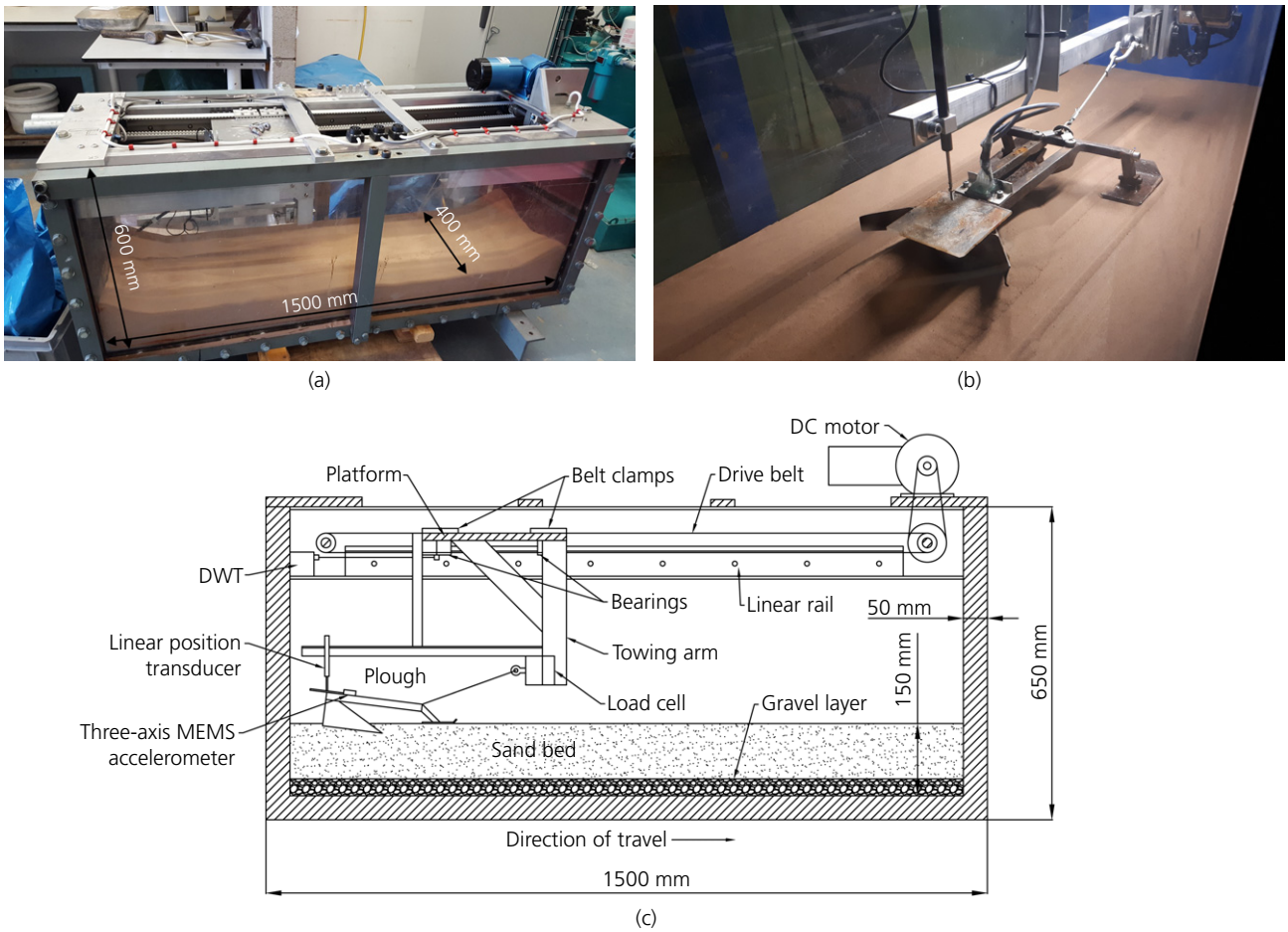

Figure 3. (a) Image of the new long centrifuge container for plough testing with the actuator mounted on top (pipeline plough omitted from container). (b) 1:50 scale model pipeline plough in apparatus at end of test. (c) Schematic cross-section of container, actuation system and instrumentation

an acceptable level and allow the actuator to provide a towing capacity of up to 5 kN, with horizontal displacements of up to 800 mm.

The design allows actual towing velocities of 14 mm/s (50 m/h), although due to the accelerated (50×) pore-pressure dissipation at 50***g*** this corresponds to a scaled plough velocity of 1 m/h if water were to be used as the pore fluid. Using hydroxypropyl methylcellulose (HPMC – Methocel) as a viscous pore fluid (300 cP) allows this scaled velocity to be increased to 300 m/h. This velocity range matches that typically used in full-scale ploughing of up to 300 m/h (Lauder *et al.*, 2013); however, in reality, velocities of up to 560 m/h may occur (Cathie and Wintgens, 2001). Increasing the Methocel viscosity further to allow this range to be investigated was not possible due to difficulties in saturating the model with the extremely viscous fluid. To overcome this, a series of additional tests with the gear ratio of the pulley system reduced to 1 were carried out, allowing scaled velocities of up to 600 m/h. This was done by changing the pulleys on the motor drive belt to be of equal diameter (78 mm).

The actuator is controlled by a DC motor speed controller, allowing the towing velocity to be set for each test, which is in turn activated by a National Instruments (NI) 9482 computer-controlled relay capable of providing 240 V mains AC power to the speed controller. The relay is mounted within an NI CompactRIO 9024 chassis, which networks the relay by way of an ethernet connection through the centrifuge's fibre optic data slip ring to a PC in the control room with a LabView interface. Hardware-based limit switches at each end of the container are used to protect the system from excessive travel in the event of a software failure.

Downloaded by [UNIVERSITY OF DURHAM] on [15/11/18]. Published with permission by the ICE under the CC-BY license

Data acquisition was provided by an eight-channel Fylde μAnalog 2 system connected to an onboard PC by USB. Instrumentation was connected to the data logger by way of an Igus E08 series e-chain to control the cabling over the full travel distance of the actuator.

3.2 Instrumentation and measurement

The horizontal displacement of the instrumentation platform was measured by a miniature Multicomp SP1-50 draw-wire transducer (DWT) mounted within the frame. Measurements of the vertical displacement of the plough were obtained from a Honeywell MLT004 linear position transducer with a 101 mm range secured to the instrumentation platform, allowing the plough depth to be measured throughout the test. The stainless-steel shaft of the position transducer rested directly above the back face of the plough on a 3 mm thick Perspex plate, which was parallel to the plough base (Figure 3(b)). This particular sensor was used due to its compact size, with the housing being only 9·5 mm in diameter and 132 mm long. The shaft was not spring loaded, and was free-falling so as not to apply additional force to the plough. The mass of the shaft was negligible at only 6·8 g. The force required to tow the plough was measured by a 5 kN Tedea Huntleigh type 616 'S' beam load cell on the towing arm, to which the plough was attached by 2·5 mm diameter stainless-steel wire rope.

Measurements of the pitch and roll of the plough provide valuable data to assess the plough performance. Lauder *et al.* (2013) used a pair of Accustar clinometers to measure rotations in the two axes, however, these had an impact on the self-weight of the plough and were not suitable for centrifuge use due to their measuring system. A replacement system for measuring plough pitch and roll was used here, based around an Analog Devices ADXL377Z three-axis accelerometer mounted on the top surface of the plough. The accelerometer measures accelerations in the x, y and z axes in the same micro-electro-mechanical systems (MEMS) sensing unit, with a measurement range of $\pm 200\boldsymbol{g}$. Coupled with the fact that it weighed only 50 g including mountings and measured 25 mm × 25 mm, the unit was ideal for centrifuge use. Technical specifications for the MEMS sensor are shown in Table 3.

Equations 3 and 4 were used to derive the pitch and roll from the measured accelerations (ADI, 2010). As the maximum horizontal acceleration of the plough at the start of the test was only 0·05 m/s^2 (four orders of magnitude lower than the enhanced gravity in the centrifuge) the impact of this dynamic effect on the pitch and roll measurements was deemed negligible. Using the Fylde Data Acquisition system, the MEMS tilt sensor provided a resolution of better than 0·05°. The accuracy of the sensor calibration could also be determined in flight by calculation of the total measured acceleration using Equation 5. Manual measurements of the orientation of the plough were taken using a hand-held inclinometer to verify the performance of the MEMS accelerometers at the start and end of the centrifuge test, and the results provided good agreement.

Table 3. Technical specifications of ADXL377Z MEMS three-axis accelerometer

Parameter	Value
Measurement range: g	±200
Shock resistance: g	±10 000
Supply voltage: V	2·5
Sensitivity: mV/g	4·24
Achievable tilt resolution: degrees	0·05
Non-linearity: %	±0·5
Temperature sensitivity: %/°C	±0·02

3. $$\text{Pitch} = \tan^{-1}\left(\frac{A_x}{\sqrt{A_y^2 + A_z^2}}\right)$$

4. $$\text{Roll} = \tan^{-1}\left(\frac{A_y}{\sqrt{A_x^2 + A_z^2}}\right)$$

5. $$\text{Total acceleration, } |A| = \sqrt{A_x^2 + A_y^2 + A_z^2}$$

4. Dry testing and sample preparation

The centrifuge tests were carried out in the Geotechnical Centrifuge Facility at the University of Dundee, using the 3 m radius beam centrifuge (Davies *et al.*, 2001; Milne *et al.*, 2012). The centrifuge is capable of applying accelerations of up to $120\boldsymbol{g}$ to model packages of 1 t, although an acceleration of $50\boldsymbol{g}$ was used for this series of tests.

The pipeline plough tested was a 1:50 scale model of a type of plough commonly used offshore (Figure 3(b)). The model plough has a mass of 1·4 kg including instrumentation, corresponding to 175 t at prototype scale. The plough is the same as that used by Lauder *et al.* (2013) in the non-forecutter case, and has a maximum possible plough depth of 40 mm (2 m at prototype scale). The depth of the plough is controlled by varying the angle of the front skid arms with a shallower angle resulting in a deeper target depth. The skid arms were accurately set to the required angle prior to each test using a Vernier protractor, before being secured using thread-lock adhesive. The front skids themselves are connected to the skid arms by a free-moving pinned connection. While the plough is

Downloaded by [UNIVERSITY OF DURHAM] on [15/11/18]. Published with permission by the ICE under the CC-BY license

set at a target depth, the actual depth achieved is dependent on the test conditions and the balance of forces on the plough share, with higher sand densities and faster velocities (in saturated tests) leading to the plough running at a shallower depth (Lauder *et al.*, 2013).

The 150 mm deep sand bed in which the plough is tested was prepared by air pluviation using a linear slot pluviator mounted on rails running above the container (relative densities from 40 to 85% were achieved). The sand bed was pluviated until a height just above the required depth was reached, before the sand surface was levelled. This was done using a Perspex surface scraper which was laser cut to the specific dimensions of the container. Next, the actuator system was placed and bolted into the container and the plough placed at the starting position.

Once the centrifuge had reached the required acceleration of 50$\boldsymbol{g}$, a rest period of 5 min was allowed to let the sensors stabilise and to minimise any creep of the sand bed. The motor relay was then activated until a typical horizontal displacement of 750 mm (37·5 m prototype) had been applied at a speed of 6 mm/s. Wireless GoPro cameras mounted on the instrumentation platform and above the container allowed the plough progress to be monitored. A further 5 min rest period was allowed before the centrifuge was spun down, and the actuator removed from the container. The final depth of the plough relative to the sand surface was measured by hand, pitch and roll of the plough relative to the container was recorded using a digital inclinometer with a resolution of 0·1°.

A new low-cost contactless three-dimensional (3D) sand surface scanning system developed as part of this research was also used to capture the final surface and trench geometry of the entire model. The system is based around a 3D systems sense 3D scanner, and is capable of generating a 3D representation of the model accurate to within ±0·5 mm. The 3D output from the system can be imported in CAD software, allowing visualisation, extraction of accurate trench cross-sections and calculations of areas and volumes. A full description of the scanning system is given by Robinson *et al.* (2016b) along with verification of its performance and accuracy. The 3D scans also allowed more accurate measurement of the final plough depths than was possible with hand measurements. This was done by applying matt adhesive tape to the Perspex platform on the top of the plough, rendering it visible to the scanner.

5. Saturated testing and sample preparation

As mentioned, while the apparatus can apply towing speeds of up to 50 m/h or 100 m/h depending on the gear ratio used, the enhanced gravity (N times) in the centrifuge caused the scaled plough velocities to be N times lower than would be achieved in a 1$\boldsymbol{g}$ test. This is due to the elevated hydraulic gradient in the pore fluid caused by the enhanced gravity, meaning that pore fluid flows and pore pressures dissipate N times faster. To account for this, a viscous pore fluid with a viscosity of N times water (1 cP) could be used to instead of water. In this case where N = 50, methylcellulose with a viscosity of 50 cP could be used to match the 1$\boldsymbol{g}$ scaled velocities. However, to extend the range of scaled plough velocities to that used offshore, methylcellulose viscosities of up to 300 cP were used to achieve scaled velocities of up to 600 m/h. The scaled plough velocity (not to be confused with the normalised velocity, V) is determined by

$$v_{\text{scaled}} = \frac{v_{\text{tow}}\eta_{\text{methocel}}}{N\eta_{\text{water}}} \quad (6)$$

where v_{scaled} is the scaled plough velocity, v_{tow} the applied towing speed, η_{methocel} the Methocel solution viscosity, η_{water} the viscosity of water and N the scaling factor, is the ratio of the enhanced gravity used relative to 1$\boldsymbol{g}$.

Viscous drag forces due to the use of methylcellulose as a pore fluid have been estimated, and found to be insignificant compared with the measured tow forces. The use of methylcellulose to modify the pore fluid viscosity in centrifuge modelling has become commonplace following studies such as Stewart *et al.* (1998). It has previously been shown that the use of highly viscous pore fluids has no significant effect on either the shear stiffness degradation (Ellis *et al.*, 2000) or the strength and stress–strain response (Zeng *et al.*, 1998) of sands.

The methylcellulose used was Alfa Aesar HPMC with a specified viscosity of 10 750 cP in 2% aqueous solution at 20°C. The relationship between solution viscosity and HPMC concentration is described by (DCC, 2002)

$$\eta = (1 + \alpha C)^8 \quad (7)$$

where η is the methylcellulose solution viscosity and C the HPMC powder concentration by mass in which the viscosity constant, α is specific to each HPMC manufacturing batch. Testing using a Brookfield LV viscometer identified the viscosity constant for the HPMC used as 1·131.

The particular grade of methylcellulose used has a higher viscosity constant than that normally used in centrifuge modelling, meaning that a lower concentration of HPMC powder is required to achieve the same solution viscosity. This had the advantage of making the mixing of the high-viscosity pore fluids easier due to the lower solids content. Methylcellulose solutions maintain a constant viscosity up to a given strain

Downloaded by [UNIVERSITY OF DURHAM] on [15/11/18]. Published with permission by the ICE under the CC-BY license

rate, after which the solution viscosity reduces as the strain rate is increased. The lower concentration of the HPMC used in this study allows this constant viscosity to be maintained at higher strain rates than possible using methylcellulose of the same viscosity prepared using a higher concentration of HPMC powder with a lower viscosity constant (DCC, 2002). This makes it well suited to use in modelling of ploughing, where high strain rates occur.

To allow full hydration of the HPMC it must be dispersed in solution at temperatures above 90°C, in which case it is insoluble. Then the solution requires to be cooled to below 20°C to fully hydrate (DCC, 2002). The solution was created in 6 litre batches by adding the required amount of HPMC with one-third of the total amount of water as boiling water and mixing for 2 min to ensure full dispersion. At this point, the remaining water was added (one third as ice and the final third at room temperature) in order to reduce the temperature to 10–15°C (below the 20°C required for hydration to start), and the solution was mixed again. This was then stored in a sealed container until required. The viscosity of the final HPMC was again checked using the viscometer once the temperature had reached room temperature and was found to vary by no more than 2% from the target viscosity.

The sand bed was prepared in the same manner as the dry tests, except with the addition of a 35 mm thick layer of gravel below the sand bed, which was covered with a layer of geotextile membrane. The overall height was kept constant meaning the sand layer was 115 mm thick. Once the model was loaded onto the centrifuge gondola and the plough and actuator were in place, the model was saturated with Methocel solution by a valve on one end of the container located at the mid-height of the gravel layer. This allows the solution to saturate the model evenly across its entire length from the base up. The saturation was carried out slowly over a period of approximately 12 h by using the valve to regulate the flow of the solution, so as not to cause uplift of the sand bed. The Methocel solution level was brought to 50 mm above the sand surface to ensure that the spoil heaps generated during ploughing remain fully covered, and the test was run in the same manner as the dry tests at the required towing speed (Table 4).

To allow surface scanning of the saturated test beds, the pore fluid was allowed to drain off at 1$\boldsymbol{g}$ until the pore fluid was below the sand surface prior to undertaking scanning as described above. This was done before the container was unloaded from the gondola in order to prevent disturbance.

6. Results

Table 4 shows the key aspects of the tests conducted, consisting of 22 centrifuge tests in total. Typical data obtained from the centrifuge tests is shown in Figures 4 and 5. This is similar to that obtained from previous 1$\boldsymbol{g}$ testing (Lauder *et al.*, 2013) and shows a transition zone where the ploughs increase in depth to their target depths, which are dictated by the skid settings. The end of the transition zone coincides with reaching a constant plough depth and near-constant tow force. Here, steady state is reached after 350 mm or 3·2 plough share lengths. Figure 5 shows this transition behaviour from the perspective of the plough kinematics where the plough inclination tends to about 0·2° (or close to zero) at transition. The inclination of the plough determined from the MEMS accelerometer system closely tracks the change in plough depth measured by the LVDT resting on the rear of the plough. The data also show that the plough is slightly deeper at its rear than the final trench depth determined post-test by the surface scanning system with a ratio of plough-to-trench depth of 0·88–0·93. This is caused by localised trench failure and the shape of the base of the plough. The plough fully transitioned to steady state within 350 mm in all tests. Once the steady-state zone is achieved this is then used to extract average tow force and plough depth for comparison of different plough tests and conditions. These key results from each of the tests are shown in Table 5.

6.1 Dry testing

The results presented in Figure 6 summarise the tow force–depth relationship for the dry centrifuge tests undertaken in loose, medium dense and very dense tests (D_r = 25–27, 44–47 and 84–85%, respectively) undertaken using the 1:50 scale plough. A fit to the data using Equation 1 has been carried out to generate values of C_s to allow comparison with the previous 1$\boldsymbol{g}$ testing. The values of C_s varying from 11·8 to 13·4 (loose to very dense) are similar to those presented by Lauder *et al.* (2013), who suggested C_s varied from 12·2 to 13·6 in loose to dense sand. The values at 1$\boldsymbol{g}$ seem slightly higher and this may be as a result of low effective stress dilation but as previously described by Lauder *et al.* (2013) and Lauder and Brown (2014) this contribution to resistance (or scaling) effects will not be as large as anticipated due to the large amount of post-peak shearing occurring once steady state has been reached. Again previous concerns over the difference between 1$\boldsymbol{g}$ model testing and field-derived C_s values are also unfounded with a similar range of limited C_s values being found during centrifuge testing. Robinson *et al.* (2017) suggested that for cable ploughs C_s could be represented by $3K_p$ or K_p^2 (similar to lateral pile consideration) where K_p is the passive earth pressure coefficient. For the sand used here at critical state using K_p^2, C_s would equal 10·6, which is close to the value of C_s between 11·8 and 13·4 found in this study.

Comparison of the centrifuge tests with the 1$\boldsymbol{g}$ tests by Lauder (2011) shows relatively good fit to the data in terms of

Downloaded by [UNIVERSITY OF DURHAM] on [15/11/18]. Published with permission by the ICE under the CC-BY license

Table 4. Summary of key aspects of centrifuge testing

Test number	Sand relative density, D_r: %	Saturation condition	Pore fluid viscosity: cP	Actuator towing speed: m/h	Scaled plough velocity: m/h	Model target depth: mm	Prototype target depth: m
SR1	44	Dry	—	22	—	23	1·15
SR2	26	Dry	—	22	—	23	1·15
SR3	84	Dry	—	22	—	23	1·15
SR4	25	Dry	—	22	—	31	1·55
SR5	26	Dry	—	22	—	16	0·80
SR6	85	Dry	—	22	—	16	0·80
SR7	27	Dry	—	22	—	35	1·75
SR8	85	Dry	—	22	—	35	1·75
SR9	46	Dry	—	22	—	35	1·75
SR10	47	Dry	—	22	—	16	0·80
SR11	85	Saturated	1	48	1	35	1·75
SR12	44	Saturated	1	48	1	35	1·75
SR14	82	Saturated	1	48	1	23	1·15
SR15	84	Saturated	100	48	96	23	1·15
SR16	88	Saturated	102	47	97	35	1·75
SR17	87	Saturated	202	47	192	35	1·75
SR18	81	Saturated	204	48	195	23	1·15
SR19	47	Saturated	201	47	191	35	1·75
SR20	45	Saturated	99	48	95	35	1·75
SR21	78	Saturated	303	96[a]	580	35	1·75
SR22	79	Saturated	198	96[a]	382	35	1·75
SR23	81	Saturated	1	101[a]	2	16	0·80

[a]Tests were conducted using reduced actuator gear ratio of 1 to allow higher towing speeds

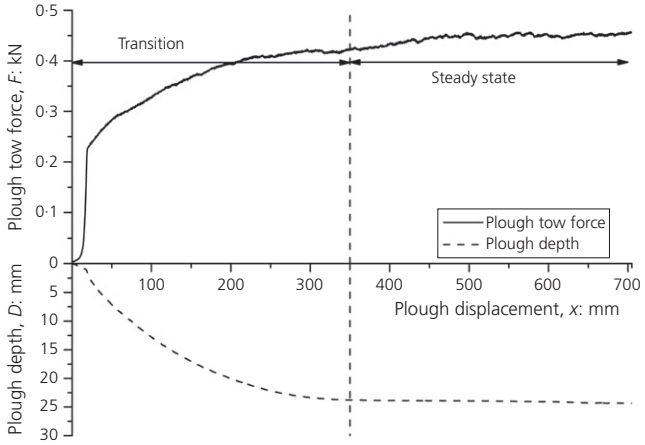

Figure 4. Variation of model plough depth and tow force with displacement during centrifuge testing in medium dense dry HST95 sand (D_r = 44%) and a target depth of 23 mm (results are shown at model scale)

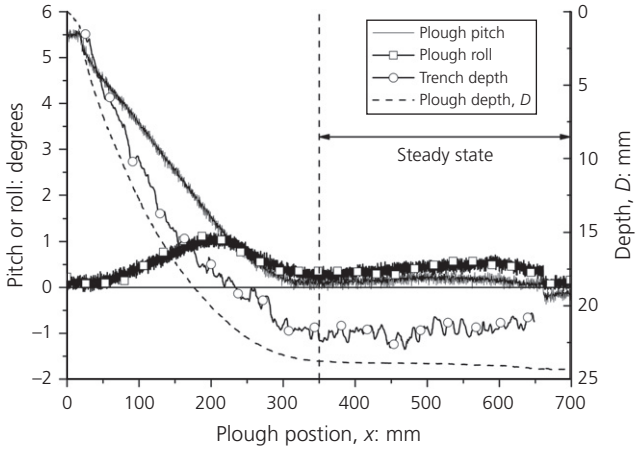

Figure 5. Variation of plough depth, pitch and trench depth during centrifuge testing in dry medium dense dry HST95 sand (D_r = 44%) and a target depth of 23 mm (results are shown at model scale)

variation of tow force with depth (Figure 7) but it appears to under predict the overall magnitude of the tow force. This is because the 1***g*** set-up used by Lauder (2011) included heavier ploughs due to the inclusion of the bulky Accustar clinometers and associated mounting details (replaced in the centrifuge testing by the lightweight MEMS accelerometer arrangement). Figure 8 shows the prototype tow force corrected for the individual plough weights (varying due to different onboard instrumentation), which suggests that the scaling used in 1***g*** testing (and proven at various scales) is appropriate. It is noted

Downloaded by [UNIVERSITY OF DURHAM] on [15/11/18]. Published with permission by the ICE under the CC-BY license

Table 5. Summary of results from centrifuge testing

Test number	Measured final depth at model scale: mm	Model steady-state tow force: kN	Measured final depth at prototype scale: m	Prototype steady-state tow force: kN
SR1	24·2	0·456	1·210	1141
SR2	27·9	0·505	1·395	1264
SR3	22·3	0·445	1·115	1113
SR4	32·2	0·659	1·610	1649
SR5	16·7	0·369	0·835	922
SR6	15·9	0·357	0·795	892
SR7	36·6	0·707	1·830	1768
SR8	33·3	0·721	1·665	1803
SR9	33·9	0·697	1·695	1743
SR10	15·9	0·364	0·795	911
SR11	33·2	0·546	1·660	1366
SR12	34·7	0·530	1·735	1324
SR14	23·0	0·370	1·150	926
SR15	21·0	0·450	1·050	1125
SR16	30·0	0·808	1·500	2021
SR17	28·7	0·971	1·435	2427
SR18	19·9	0·526	0·995	1314
SR19	29·6	0·822	1·480	2055
SR20	35·1	0·666	1·755	1665
SR21	24·6	1·081	1·230	2703
SR22	28·2	0·958	1·410	2396
SR23	15·2	0·318	0·760	795

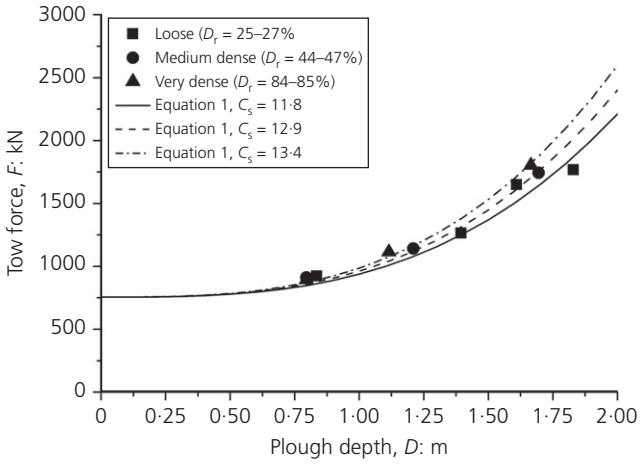

Figure 6. Results of centrifuge testing in dry HST95 sand at various relative densities and depth shown fitted by the Cathie and Wintgens (2001) equation with updated passive pressure coefficient values (results are shown at prototype scale)

that the 1:10 scale plough tests show increased shallow depth tow force but become better at increasing depth. This was due to subtle shape differences between the shapes of the base of the plough running from the heel to the toe. These differences in manufacture were not noticed until after testing and highlight the necessity for strict quality control on model manufacture when using models of different scales.

By obtaining very similar values using the two testing methods and various scales, these data show that parameter C_s may be derived from 1g testing without significant errors induced by the low effective stress levels in these tests.

6.2 Saturated testing

To investigate the velocity dependence on plough performance, tests were carried out at a range of normalised velocities as summarised in Table 4, using the method described above. It was decided to limit the testing for rate effects investigation to medium dense and very dense sand due to limited centrifuge access time and the required number of repeat tests. Figure 9 shows the results of saturated testing in medium dense and very dense sand. It is clear that the rate effect increases significantly with increasing depth in the very dense sand (with initial target depths of 23 and 33 mm, respectively). The nonlinear increase in the tow force with plough speed is a result of the plough tending to reduce in depth as tow force increases to maintain moment equilibrium (Brown *et al.*, 2015). Figure 10 compares the normalised force or rate effect with the normalised plough velocity as proposed by Lauder *et al.* (2012) with data presented from the previous 1g testing (Figure 2). It can be seen that there is considerable scatter in the data with the dynamic rate effect coefficient determined for the centrifuge tests (C_{dn} = 12·3) being significantly lower than the values

Downloaded by [UNIVERSITY OF DURHAM] on [15/11/18]. Published with permission by the ICE under the CC-BY license

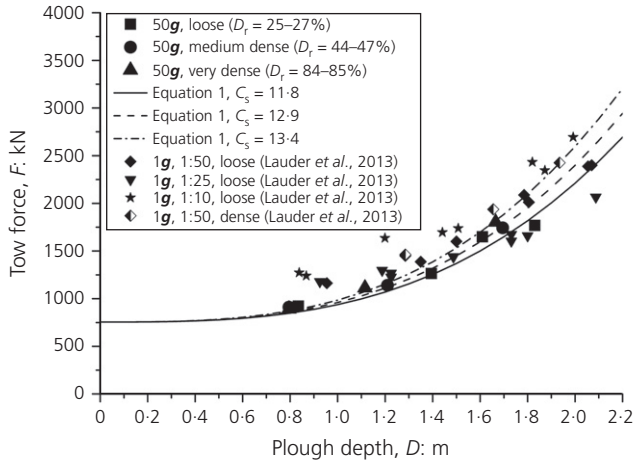

Figure 7. Comparison of the centrifuge testing with the previous 1***g*** testing undertaken by Lauder *et al.* (2013) (results shown at prototype scale)

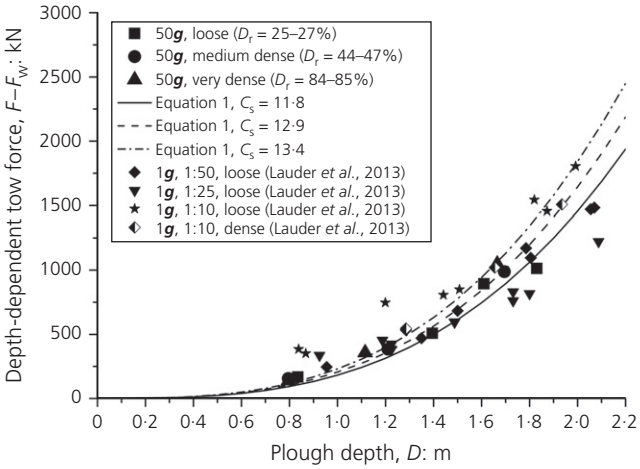

Figure 8. Comparison of the dry centrifuge testing with the previous 1***g*** testing undertaken by Lauder *et al.* (2013) with the tow force results corrected for variations in plough weight (results shown at prototype scale)

previously associated with 1***g*** tests (C_{dn} = 20·4). The scatter in the data although is as a result of the change in depth during ploughing, which reduces with increasing tow force and results in lower values of $F_{v=0}$ with increasing rate of testing (Figure 11). Thus, the normalisation of the tow force based on the static force at the target depth is not appropriate and this calculation needs to reflect the steady-state depth during the tests ($F^*_{v=0}$). Figure 12 shows similar data but with the normalised force calculated based on the relationship derived in Figure 11. The best-fit lines to the corrected 1***g*** data and

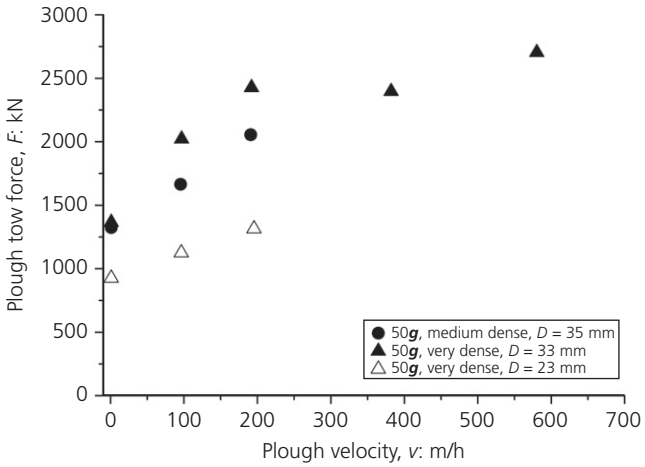

Figure 9. Effect of plough velocity on the measured tow force during centrifuge testing in saturated HST95 sand at various relative densities and with different plough target depths (results shown at prototype scale)

centrifuge data result in very consistent average behaviour with C_{dn} values of 20·4 and 19·8, respectively. One significant outlier point although is still apparent for the medium dense test at 35 mm target depth. This test was disturbed during handling and after saturation, resulting in (unknown) positive pore pressures and subsequent consolidation to a lower voids ratio resulting in an unknown dilation potential (s in Equation 2). It is anticipated that the sand would have densified and would thus have a higher value of s and would therefore be consistent with the other data shown in Figure 12. After that all other centrifuge tests were saturated on the centrifuge arm to minimise handling effects.

7. Summary and conclusions

To verify scaling assumptions prior to further small 1***g*** ploughing investigations, the equipment was developed to allow this large displacement event to be simulated on a medium-sized beam centrifuge using a specially developed long centrifuge box and actuation system. This system was capable of plough tests of 800 mm displacement, which was adequate to allow plough transition and determined steady-state behaviour. With the use of the purpose-built actuation it was possible to achieve scale velocities of 1 m/h using water and through the use of methycellulose solution it was possible to increase this much further to 600 m/h to study the scaling of rate effects over the range of speeds normally encountered during real ploughing projects. This testing was further enhanced through the use of MEMS accelerometers to measure plough pitch and roll and a newly developed low-cost 3D sand surface scanning technique.

Downloaded by [UNIVERSITY OF DURHAM] on [15/11/18]. Published with permission by the ICE under the CC-BY license

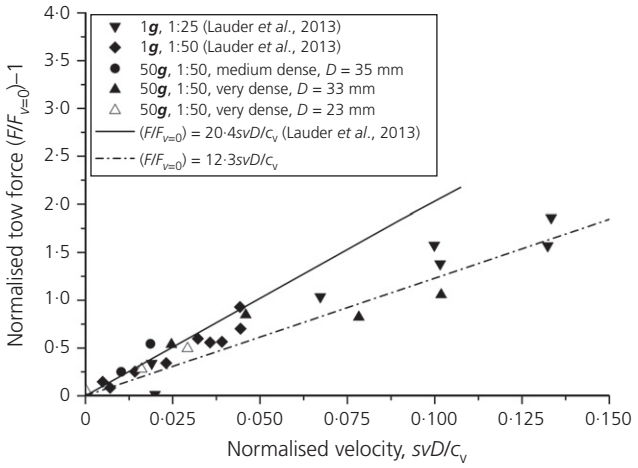

Figure 10. Comparison of normalised rate effect behaviour for the previous 1***g*** and 50***g*** centrifuge testing

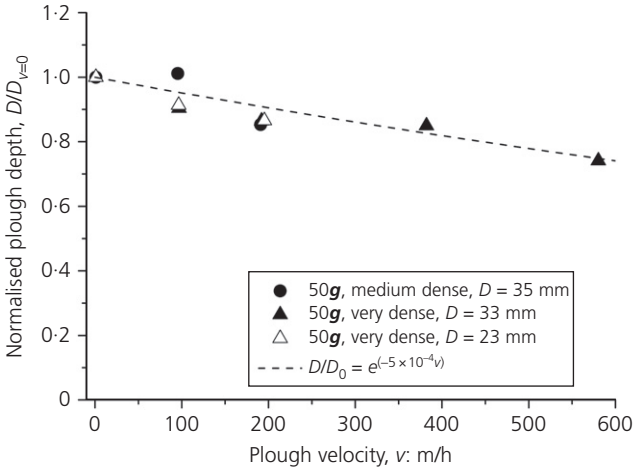

Figure 11. Reduction of normalised plough depth with increasing plough velocity from saturated centrifuge testing in very dense and medium dense HST95 sand

The results of this centrifuge study have verified that in the case of offshore ploughing it is possible to use small-scale ploughs at 1***g*** even in very dense sands without encountering significant difficulties with dilation effects. It also shows that previously proposed methods of scaling are valid at 1***g*** although care needs to be taken during rate effects studies to consider the appropriate depth of the plough during testing as this may vary significantly from target depths due to increased rate-dependent tow forces. The study shows that there are significant benefits in physical modelling of complex full-scale events where it is difficult to deconvolute behaviour. This has led to verification of improved parameters for the prediction of pipeline plough performance.

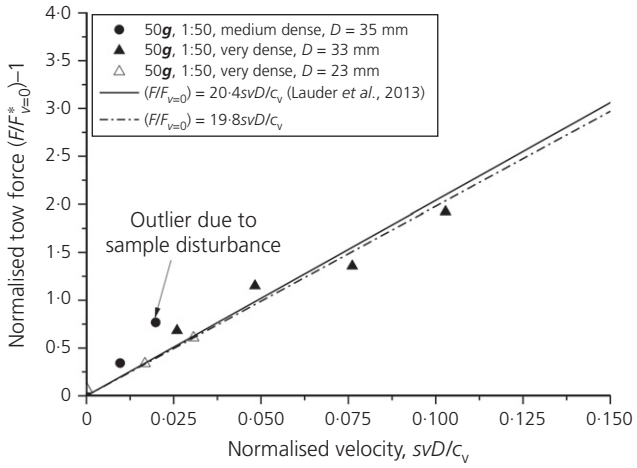

Figure 12. Comparison of normalised rate effect behaviour for the previous 1***g*** and 50***g*** centrifuge testing with normalised tow force corrected for plough depth changes that occur with increasing plough speed

Acknowledgements

The model seabed ploughing described in this paper has been undertaken for the EPSRC funded project Seabed ploughing: modelling for infrastructure installation (EP/M000362/1 and EP/M000397/1). The 3D surface scanning technique and centrifuge ploughing actuation systems have been developed as part of the Scottish Marine and Renewables Test (SMART) Centre at the University of Dundee, funded by the European Regional Development Fund (ERDF).

REFERENCES

ADI (Analog Devices Inc.) (2010) *Application Note AN-1057: Using an Accelerometer for Inclination Sensing*. Analog Devices Inc., Norwood, MA, USA. Available at: http://www.analog.com/media/en/technical-documentation/application-notes/AN-1057.pdf (accessed 30/10/2017).

Bransby MF, Yun GJ, Morrow D and Brunning P (2005) The performance of pipeline ploughs in layered soils. In *Proceedings of the International Symposium on Frontiers in Offshore Geotechnics (ISFOG 2005)* (Gourvenec S and Cassidy M (eds)). CRC Press, Perth, Western Australia, Australia, pp. 597–606.

Bransby MF, Brown MJ, Hatherley A and Lauder K (2010a) Pipeline plough performance in sand waves. Part 1: model testing. *Canadian Geotechnical Journal* **47(1)**: 49–64. https://doi.org/10.1139/T09-077.

Bransby MF, Brown MJ, Lauder K and Hatherley A (2010b) Pipeline plough performance in sand waves. Part 2: kinematic calculation method. *Canadian Geotechnical Journal* **47(1)**: 65–77. https://doi.org/10.1139/T09-091.

Downloaded by [UNIVERSITY OF DURHAM] on [15/11/18]. Published with permission by the ICE under the CC-BY license

Bransby MF, Barlow D, Brown MJ *et al.* (2018) The performance of pipeline ploughs traversing seabed slopes. *Ocean Engineering Journal* **148**: 125–135. https://doi.org/10.1016/j.oceaneng.2017.11.028.

Brown MJ, Bransby MF and Simon-Soberon F (2006) The influence of soil properties on ploughing speed for offshore pipeline installation. In *Proceedings of the 6th International Conference on Physical Modelling in Geotechnics (ICPMG'06)* (Ng CW, Zhang LM and Wang YH (eds)). CRC Press, Hong Kong, China, pp. 709–714.

Brown MJ, Bransby MF, Knappett JA *et al.* (2015) The effect of buried fibres on offshore pipeline plough performance. *Ocean Engineering Journal* **108**: 760–768. https://doi.org/10.1016/j.oceaneng.2015.08.022.

Cathie DN and Wintgens JF (2001) Pipeline trenching using plows: performance and geotechnical hazards. *Proceedings of the 33rd Annual Offshore Technology Conference (OTC) (13145), Houston, TX, USA*, pp. 1–14.

Cortis M, Coombs WM, Augarde CE *et al.* (2017) Modelling seabed ploughing using the material point method. *Procedia Engineering* **175**: 1–7. https://doi.org/10.1016/j.proeng.2017.01.002.

Davies MCR, Newson TA and Bransby MF (2001) Geotechnical centrifuge modelling at the University of Dundee. *Proceedings of the International Symposium on Geotechnical Centrifuge Modelling and Networking*. CRC Press, Hong Kong, China, pp. 15–16.

DCC (Dow Chemicals Company) (2002) *Methocel Cellulose Ethers: Technical Handbook*. Dow Chemical Company, Midland, MI, USA.

Ellis EA, Soga K, Bransby MF and Sato M (2000) Resonant column testing of sands with different viscosity pore fluids. *Journal of Geotechnical and Geoenvironmental Engineering* **126(1)**: 10–17.

Garnier J, Gaudin C, Springman SM *et al.* (2007) Catalogue of scaling laws and similitude questions in geotechnical centrifuge modelling. *International Journal of Physical Modelling in Geotechnics* **7(3)**: 1–23. https://doi.org/10.1680/ijpmg.2007.070301.

Grinsted TW (1985) *Earthmoving in Submerged Sands*. PhD thesis, University of Newcastle, Newcastle, UK.

Lauder KD (2011) *The Performance of Pipeline Ploughs*. PhD thesis, University of Dundee, Dundee, UK.

Lauder K and Brown MJ (2014) Scaling effects in the 1***g*** modelling of offshore pipeline ploughs. In *Proceedings of the 8th International Conference on Physical Modelling in Geotechnics (ICPMG'14)* (Gaudin C and White D (eds)). CRC Press, Perth, Western Australia, Australia, pp. 377–383.

Lauder K, Brown MJ, Bransby MF and Gooding S (2012) The variation of tow force with velocity during offshore ploughing in granular materials. *Canadian Geotechnical Journal* **49(11)**: 1244–1255. https://doi.org/10.1139/t2012-086.

Lauder K, Brown MJ, Bransby MF and Boyes S (2013) The influence of incorporating a forecutter on the performance of offshore pipeline ploughs. *Applied Ocean Research Journal* **39**: 121–130. https://doi.org/10.1016/j.apor.2012.11.001.

Milne FD, Brown MJ, Knappett JA and Davies MCR (2012) Centrifuge modelling of hillslope debris flow initiation. *Catena* **92**: 162–171. https://doi.org/10.1016/j.catena.2011.12.001.

OSIG (Offshore Site Investigation and Geotechnics Group) (2004) *Offshore Soil Investigation Forum. Guidance Notes on Geotechnical Investigations for Marine Pipelines. Offshore Site Investigation and Geotechnics Group (OSIG) Report*. Society for Underwater Technology (SUT), London, UK.

Palmer AC (1999) Speed effects in cutting and ploughing. *Géotechnique* **49(3)**: 285–294.

Reece AR and Grinsted TW (1986) Soil mechanics of submarine ploughs. *Proceedings of the Eighteenth Annual Offshore Technology Conference, Houston, TX, USA*, pp. 453–461.

Robinson S, Brown MJ, Brennan AJ *et al.* (2016a) Improving seabed cable plough performance for offshore renewable energy. In *Proceedings of the 2nd International Conference on Renewable Energies Offshore (Renew 2016) Lisbon, Portugal* (Guedes Soares C (ed.)). Taylor & Francis, London, UK, pp. 413–419.

Robinson S, Brown MJ, Brennan AJ *et al.* (2016b) Development of low cost 3D soil surface scanning for physical modelling. In *Proceedings of the 3rd European Conference on Physical Modelling in Geotechnics (Eurofuge 2016), Nantes, France* (Thorel L, Bretschneider A, Blanc M and Escoffier S (eds)), pp. 159–164.

Robinson S, Brown MJ, Brennan AJ *et al.* (2017) Improvement of seabed cable plough tow force prediction models. *Proceedings of the 8th International Conference on Offshore Site Investigation & Geotechnics (SUT OSIG), London, UK*. Society for Underwater Technology (SUT), UK, pp. 914–921.

Stewart DP, Chen YR and Kutter BL (1998) Experience with the use of methylcellulose as a viscous pore fluid in centrifuge models. *Geotechnical Testing Journal* **21(4)**: 365–369.

Zefirova A, Brown MJ, Brennan A and Boyes S (2012) Improving the performance of offshore pipeline ploughs using vibration. In *Proceedings of the 7th International Conference on Offshore Site Investigation & Geotechnics (SUT OSIG), London, UK* (Allan P, Arthur J, Barwise A *et al.* (eds)). Society for Underwater Technology (SUT), UK, pp. 395–401.

Zeng X, Wu J and Young B (1998) Influence of viscous fluids on properties of sand. *Geotechnical Testing Journal* **21(1)**: 45–51.

How can you contribute?

To discuss this paper, please email up to 500 words to the editor at journals@ice.org.uk. Your contribution will be forwarded to the author(s) for a reply and, if considered appropriate by the editorial board, it will be published as discussion in a future issue of the journal.

International Journal of Physical Modelling in Geotechnics relies entirely on contributions from the civil engineering profession (and allied disciplines). Information about how to submit your paper online is available at www.icevirtuallibrary.com/page/authors, where you will also find detailed author guidelines.

Downloaded by [UNIVERSITY OF DURHAM] on [15/11/18]. Published with permission by the ICE under the CC-BY license